Reproduced from Agronomy Journal. Published by American Society of Agronomy. All copyrights reserved.

Using the CROPGRO-Peanut Model to Quantify Yield Gaps of Peanut in the Guinean Savanna Zone of Ghana

J. B. Naab, Piara Singh, K. J. Boote,* J. W. Jones, and K. O. Marfo

ABSTRACT

Peanut (*Arachis hypogaea* L.) yield in Ghana is limited by variable rainfall, low soil fertility, pests and diseases, and poor crop management. Field experiments were conducted during the 1997 and 1998 seasons at the Savanna Agricultural Research Station in Ghana to evaluate the CROPGRO-peanut model for its ability to simulate growth, yield, and soil water balance of a peanut crop and to quantify yield losses caused by biotic and abiotic factors. Two peanut cultivars, Chinese which matures in 90 d, and F-Mix which matures in 120 d, were grown rainfed on an Alfisol soil at three sowing dates between May and August in 1997 and at four dates in 1998. Soil water and crop growth were measured during the season and compared with crop model simulations to determine yield-limiting factors relative to potential yield. Growth and yield were highest for the early sowing dates and decreased progressively with later sowing, a trend attributed to leaf diseases. After incorporating functions for percentage leaf defoliation and percentage diseased leaf area, the model accurately simulated soil water content fluctuations, crop growth, and yield of cultivars for the sowing dates and seasons. Simulated yield losses caused by water deficits were small (averaging 5–10%) for early sowing dates (late May to mid-July) and increased with later sowing dates (20 and 70% for third and fourth sowings). Yield losses due to diseases and pests were simulated as a percentage of potential yield under water-limited environments and averaged 40%, also increasing with later sowing dates. Using 13 yr of weather data, simulated yields were reduced 10 to 20% by water deficit for the two earlier (normal) sowing dates, but more for the later sowing dates, while additional yield reductions were attributed to biotic stresses. We conclude that the CROPGRO-peanut model can be successfully used to quantify the yield potential and yield gaps associated with yield-reducing stresses and crop management for this region.

Peanut is an oil seed crop commonly cultivated by farmers in Northern Ghana. About 185 000 ha of land is under peanut cultivation with average yield of about 0.85 t/ha (FAO, 1997). Production is mainly rainfed. Annual rainfall varies from 800 to 1200 mm, which should be adequate for peanut production. But there is considerable variability in the amount and distribution of rainfall, both within and between seasons, giving droughts of varying lengths and severity causing farmers' yields to be below the expected yields. At the onset of the season, rainfall is erratic such that very early sowing can be risky, often resulting in plants emerging during a period of drought. On the other hand, late sowing may increase risk of water deficit at critical pod-filling stages of the crop if the season is short. Yield losses from diseases such as early leafspot (*Cercospora arachidicola*), late leafspot (*Cercosporidum personatum*), rosette virus, and rust (*Puccinia arachidis* Speg.) are also prevalent because peanut farmers in West Africa do not use disease control measures. The soils of the region generally have low fertility and low water-holding capacity, both contributing to lower yields.

Identifying major yield-limiting factors and appropriate agronomic management practices for increasing peanut production through field experimentation may involve many years of data collection on which to make meaningful deductions. This is time consuming and expensive. In recent years, crop models have increasingly been used to support breeding research, field agronomic advice, and even decision support for agricultural policy formulation (Boote et al., 1996). Crop models can also be used to determine potential yields for a site based on the weather conditions and soil water-holding characteristics of the site, and then a systems approach can be taken to determine causes of, and possible remedies for minimizing, the yield gap between the potential and the realized yields. Experiences in India with crop model analyses relative to peanut experiments indicated substantial "yield gaps" not associated with climatic limitations (Singh et al., 1994). Experience with model analyses of peanut growth in on-farm trials in Florida, USA (Gilbert, 1992; Gilbert et al., 2002), showed yield gaps in approximately half of the farmers' fields caused by biotic stresses including rootknot nematode (*Meloidogyne arenaria*), *Cercospora* leafspot, and white mold (*Sclerotium rolfsii*). Systems models along with short-term field experiments can be used to quantify yield losses associated with biotic stress, abiotic stresses, and poor crop management.

Once a crop model is tested and validated for a given site, it can be used with long-term historical weather data to simulate crop performance under varying cultural practices such as sowing dates, sowing densities, cultivar selection, soil fertility, and diseases. Crop models can then be used to analyze the impact of these factors on production over a broader region and broader range of seasons. With this information, researchers can then focus on the major yield-limiting factors and give better advice to producers.

The CROPGRO-peanut model (Boote et al., 1998)

J.B. Naab, Savanna Agric. Res. Inst., Tamale, Ghana; P. Singh, Int. Crops Res. Inst. for the Semi-Arid Tropics (ICRISAT), Patancheru, Andra Pradesh 502 324, India; K.J. Boote, Dep. of Agron., Univ. of Florida, Gainesville, FL 32611-0500; J.W. Jones, Dep. of Agric. and Biol. Eng., Univ. of Florida, Gainesville, FL 32611-0500; and K.O. Marfo (deceased), Savanna Agric. Res. Inst., Tamale, Ghana. This research was supported in part by the United States Agency for International Development, Peanut Collaborative Research Support Project. Florida Agric. Exp. Stn. Journal Ser. no. R-09285. Received 28 Jan. 2003. *Corresponding author (kjb@mail.ifas.ufl.edu).

Published in Agron. J. 96:1231–1242 (2004).
© American Society of Agronomy
677 S. Segoe Rd., Madison, WI 53711 USA

Abbreviations: CN2, runoff curve number; DUL, drained upper limit; LL, lower limit of plant available water; PESW, plant extractable soil water; RMSE, root mean square error; SAT, saturated upper limit; SWCON, fraction of water above field capacity drained per day; WR, root weighting function.

Reproduced from Agronomy Journal. Published by American Society of Agronomy. All copyrights reserved.

is the most recent version of the PNUTGRO model (Boote et al., 1986, 1989b, 1991), which has been steadily improved since 1986. This model was tested in India (Singh et al., 1994) and with on-farm trials in Florida (Boote et al., 1989a; Gilbert, 1992; Gilbert et al., 2002). Between 1990 and 1994, more mechanistic features of leaf-level photosynthesis, hedge-row canopy photosynthesis, explicit N_2–fixation, explicit soil N uptake, and soil N balance were added, and the CROPGRO-legume model was released (Hoogenboom et al., 1992, 1993, 1994). This version simulates three grain legumes {soybean [*Glycine max* (L.) Merr.], peanut, and bean (*Phaseolus vulgaris* L.)} with one common FORTRAN code and follows the standard input/output protocols of the DSSAT (Decision Support System for Agrotechnology Transfer) (IBSNAT, 1989). Species parameters and cultivar traits are entered as external input files. Boote et al. (1998) described how CROPGRO (version 3.5, 1998 release) simulates the daily processes of crop development, crop C balance, crop and soil N balance, and soil water balance. This model also has coupling points and procedures for entering pest damage to simulate hypothetical growth and yield reductions due to such factors as percentage leaf area defoliation or percentage necrosis (Batchelor et al., 1993; Boote et al., 1993).

The objectives of the field study conducted at Nyankpala, Ghana, were (i) to evaluate the ability of the CROPGRO-peanut crop growth model (Version 3.5) to simulate peanut growth, yield, and soil water balance under rainfed conditions of Northern Ghana and (ii) to use the model to estimate climatic potential yields and yield losses caused by inadequate water availability, diseases, and management practices.

MATERIALS AND METHODS

Field Experiments

The experiments were conducted in 1997 and 1998 at the Savanna Agricultural Research Institute located at Nyankpala (9°42′ N, 0°55′ W; 184 m elevation) near Tamale, Ghana. The soil was a sandy loam alfisol about 1.2 m deep with 100 to 110 mm of maximum plant extractable soil water (PESW).

The experiments consisted of six or eight treatments as factorial combination of three or four sowing dates and two peanut cultivars. In 1997, the three sowing dates were 29 May (D1), 26 June (D2), and 24 July (D3). In 1998, the four sowing dates were 22 May (D1), 19 June (D2), 20 July (D3), and 17 August (D4). Two improved cultivars were selected, Chinese which matures in 90 d, and F-mix which matures in 120 d. Chinese is the recommended short-season cultivar and is widely grown by farmers, and F-mix is a recommended longer-season cultivar with higher yield potential. A randomized complete block design with four replications was used each year. Individual plot size measured 8 by 4.5 m (eight rows). Seeds were sown by hand at 4-cm depth in a flat seedbed in 0.50-m row spacing and 0.10-m spacing between plants.

Before sowing each year, the field was disc-plowed to a depth of 0.15 m and harrowed. At sowing in 1997, P as single superphosphate and K as KCl were applied at 60 kg P_2O_5 and 30 kg K_2O per hectare. In 1998, no fertilizers were applied. Weeds were controlled using a pre-emergence herbicide, a pre-package mix of acifluorfen {5-[2-chloro-4-(trifluoromethyl)phenoxy]-2-nitrobenzoic acid} plus bentazon [3-(1-methylethyl)-1*H*-2,1,3-benzothiadiazin-4(3*H*)-one 2,2-dioxide] (at 0.28 + 0.56 kg a.i. ha^{-1}), and hand hoeing as needed.

Measurements

Soil water content was measured at 6- to 10-d intervals, more frequently after major rain events, during each season using a Troxler 3330 neutron probe calibrated for the experimental site. One aluminum access tube was installed in each plot to a depth of 1.10 m. Probe readings were taken at 0.15-m-depth intervals beginning at 0.30 m, down to a depth of 1.10 m. Water content of the top 0.15- and 0.15- to 0.30-m layers was determined by gravimetric methods and volumetric water contents calculated using bulk densities measured for this soil.

Phenology observations were taken at weekly intervals to determine days to 50% of plants at emergence, flowering, beginning peg (first gynophore elongated toward the soil), first mature pod, harvest maturity (70–80% mature pods), and number of nodes on the main stem following the peanut growth staging of Boote (1982). Total dry matter accumulation and partitioning into leaves, stems, and pods were determined at 10- to 14-d intervals, based on plants from two adjacent 1.0-m lengths of row (1.0-m^2 land area). Plants were separated into leaves, stems, and pods, which were oven-dried at 70°C for 48 h and weighed.

At final harvest, pods from bordered inner rows (8-m^2 land area) were hand-harvested from each plot. The pods were air-dried, weighed, and shelled. The shell and seed weights were also determined.

A rain gauge was installed at the experimental site to collect rainfall data. Daily maximum and minimum temperatures and bright sunshine hours were measured at a weather station situated 1 km from the experimental site. Solar radiation (MJ/m^2) was estimated from bright sunshine hours using the WEATHERMAN utility program of DSSAT v 3 software (Hansen et al., 1994).

All the data on climate, soil, crop growth, and yields collected for the two seasons were entered in the standard file formats (*.PNX, *.PNA, *.PNT, *.WTH, and SOIL.SOL) needed for execution of the CROPGRO-peanut model.

Model Calibration

Soil Water Balance and Soil Water-Holding Characteristics

The soil water balance submodel used in CROPGRO is described in detail by Ritchie (1985). In the model, volumetric water content in each soil layer varies between a lower limit (LL) and a saturated upper limit (SAT). If water content of a given layer is above the drained upper limit (DUL), then water is drained to the next layer with the "tipping bucket" concept, using a drainage coefficient specified for the soil. Infiltration and runoff of rainfall depend on the U.S. Soil Conservation Service runoff curve number (CN2). The model uses the method of Priestley and Taylor (1972) to estimate potential evapotranspiration. Potential plant transpiration is computed as an asymptotic function of leaf area index and the potential evapotranspiration. Water-supplying capacity of the soil–root system is calculated from root length and soil water content in each layer and then compared against climatic potential transpiration. Actual transpiration is the minimum of the two rates.

The soil water-holding characteristics required by the model [DUL, LL, SAT, runoff, drainage fraction, Stage 1 evaporation (U), etc.] were initially estimated by inputting soil texture (percentage sand, silt, and clay) and other information such as bulk density and soil organic matter into a soil file creation utility program of the DSSAT software. These estimated characteristics for the soil were further modified to make them more specific for the experimental site, following the procedure of Singh et al. (1994) described here. Frequent (6–10 d) monitoring of soil water during the season allowed us to refine

Reproduced from Agronomy Journal. Published by American Society of Agronomy. All copyrights reserved.

Table 1. Soil characterization: drained upper limit (DUL), lower limit of plant available water (LL), root length density weighting factor for each depth (WR, unitless), limit of first-stage soil water evaporation (U), runoff curve number (CN2, unitless), and soil water drainage coefficient (SWCON) used for model simulations for respective sowing dates and seasons.

	1997 Sown 29 May			1997 Sown 26 June and 24 July			1998 All sowing dates		
Soil depth	DUL	LL	WR	DUL	LL	WR	DUL	LL	WR
cm	—— $cm^3\ cm^{-3}$ ——			—— $cm^3\ cm^{-3}$ ——			—— $cm^3\ cm^{-3}$ ——		
0–5	0.257	0.095	1.00	0.257	0.095	1.00	0.247	0.060	1.00
5–15	0.227	0.060	1.00	0.227	0.060	1.00	0.227	0.050	1.00
15–30	0.228	0.060	0.70	0.228	0.060	0.70	0.228	0.050	0.70
30–45	0.229	0.105	0.35	0.229	0.105	0.35	0.229	0.105	0.35
45–60	0.205	0.120	0.25	0.216	0.120	0.25	0.205	0.120	0.25
60–90	0.200	0.130	0.05	0.216	0.130	0.05	0.200	0.130	0.05
90–113	0.197	0.130	0.02	0.216	0.130	0.02	0.197	0.130	0.02
	U	CN2	SWCON	U	CN2	SWCON	U	CN2	SWCON
	mm		fraction drained d^{-1}	mm		fraction drained d^{-1}	mm		fraction drained d^{-1}
	6.0	76.0	0.40	6.0	76.0	0.65	6.0	78.0	0.65

the estimate of DUL for each soil layer by examining changes in water content with time after sufficient wetting by rains and identifying periods when soil water content remained constant for three or more days. Thus, DUL represents water content at field capacity, after time for free drainage. Similarly, the LL to which plants can extract soil water was estimated for each layer by identifying the lowest water content during drying cycles similar to the approach of Ritchie (1985), except for the deepest layers from which water uptake was negligible. For these deeper layers, we assumed that DUL and LL did not differ greatly from the layers above having similar bulk density and texture. The value of the upper limit of U was adjusted if soil water content for the top 5-cm layer declined too fast or slow soon after complete wetting. If simulated water contents in the deeper layers were underestimated following rains after a long drying cycle, the runoff coefficient (CN2) was decreased, and the drainage coefficient (SWCON, fraction of water above field capacity drained per day) was increased to percolate more water in the subsoil. If deeper water contents were overestimated, the curve number was increased to decrease infiltration and the drainage coefficient decreased to slow down percolation of water in the soil profile such that the simulated soil water contents matched the observed data for both the top and subsoil layers. To set the depth and shape of water extraction by the root system from soil profile depth zones, changes were made in the root weighting functions (WR) for each soil layer such that soil water extraction from each soil layer matched the observed data. Increasing the value of WR increased the water extraction and vice-versa. We had a limited amount of measured root length density data vs. soil depth that was also used to adjust WR. Table 1 lists the calibrated soil characteristics, after following this somewhat iterative procedure.

Calibration of Genetic Coefficients

The CROPGRO-peanut model requires genetic coefficients that describe durations of phases of the crop life cycle, vegetative growth traits, and reproductive traits unique to a given cultivar (Boote et al., 1998). As these were not available for the cultivars used in these experiments, peanut cultivars TMV 2 and Robut 33-1 were used as starting points from which to calibrate Chinese and F-Mix cultivars, respectively. Genetic coefficients (Table 2) were determined by iteration of model simulation against data from 1997, in the following order, as described by Boote et al. (1999). First, coefficients for duration to flowering (EM-FL), beginning pod (FL-SH), beginning seed (FL-SD), and maturity (SD-PM) were adjusted to predict the observed life cycle. The Chinese cultivar flowered and matured sooner and had a smaller photothermal day (PD) requirement for emergence to beginning bloom than F-mix (17 vs. 19 PD). Photothermal day requirements listed in Table 2 are equivalent to calendar days, if the temperature is at the optimum 28°C for the entire 24-h day, where peanut's base and optimum temperatures are 11 and 28°C, respectively. The coefficients for flower to first seed (FL-SD) and first seed to maturity (SD-PM) were adjusted to reproduce duration of growth stages observed by peanut breeders for these cultivars, causing simulated maturity near the time of actual harvest. F-mix is a longer life cycle cultivar, having longer photothermal requirements after flowering (FL-SD of 19 PD and SD-PM of 70.5 PD, Table 2). The coefficients for rate of node appearance

Table 2. Genetic coefficients of cultivars Chinese and F-mix used for model simulations.

Genetic coefficient	Abbreviation	Chinese	F-mix
Photothermal days from emergence to flower appearance	EM-FL	17.0	19.0
Photothermal days from beginning flower to beginning pod	FL-SH	7.0	8.8
Photothermal days from beginning flower to beginning seed	FL-SD	17.5	19.0
Photothermal days from beginning seed to maturity	SD-PM	53.00	70.5
Photothermal days from begin flower to end of leaf expansion	FL-LF	70.0	77.0
Maximum leaf photosynthesis rate, mg $CO_2\ m^{-2}\ s^{-1}$	LFMAX	1.24	1.24
Specific leaf area, $cm^2\ g^{-1}$	SLAVAR	275	270
Maximum size of full leaf, cm^2	SIZELF	20.0	19.0
Maximum fraction of daily growth partitioned to seed + shell	XFRUIT	0.78	0.77
Maximum weight per seed, g	WTPSD	0.36	0.45
Photothermal days for seed filling per individual seed	SFDUR	29.0	36.0
Average seed numbers per pod, no. pod^{-1}	SDPDV	1.65	1.65
Photothermal days to reach full pod load	PODUR	14.0	25.0
Number of main-stem nodes produced per photothermal day	TRIFOL	0.35	0.34
Relative plant height	RHIGHT	0.85	0.60
Relative plant width	RWIDTH	0.80	0.75

Reproduced from Agronomy Journal. Published by American Society of Agronomy. All copyrights reserved.

(TRIFOL) and relative canopy width and height (RWIDTH and RHIGHT) were set from vegetative stage, width, and height over time. The soil fertility factor (SLPF) was modified to fit the slope of dry matter accumulation of the cultivars, visually averaging over all sowing dates. The modified SLPF value was 0.86, which is less than the standard SLPF of 0.92 used for simulations in Florida, USA. Thus the "fertility" yield gap could be viewed as 6%. A parameter for rate of early leaf area growth (SIZELF) was changed to mimic rate of early-season dry matter gain. Reproductive coefficients for the timing of pod set, seed set, rate of pod addition, maximum partitioning intensity to pods-seeds, and single seed fill duration (FL-SH, FL-SD, PODUR, XFRUIT, SFDUR) were modified to simulate pod and seed growth, especially the time series of pod harvest index. Some of these genetic coefficients, especially those determining vegetative growth and reproductive growth duration, were set in an initial iteration before the calibration of soil water-holding characteristics and then later adjusted again after soil water-holding characteristics were fixed.

Statistical Evaluation of Model Performance

To evaluate model performance and accuracy in prediction, statistical indicators of root mean square error (RMSE) and the Willmott (1981) index of agreement (*d* value) were computed from observed and simulated variables (soil water content, pod harvest index, leaf mass, pod mass, and total crop biomass). The Willmott (1981) *d* value is a better indicator of model performance, particularly relative to 1:1 line, than a correlation coefficient (r or r^2), and values closer to 1 indicate better prediction while a *d* value of zero indicates no predictability.

RESULTS AND DISCUSSION

Weather

The 1997 season was cooler and received more rainfall than the 1998 season (Table 3). Mean monthly minimum temperatures from May to December remained below 23°C during 1997, whereas during 1998 season, the minimum temperatures ranged from 24 to 26°C. Earlier sowings during 1998 suffered more from water deficits during the season than did the late sowings. The crop during 1997 did not suffer from any significant water deficits, based on model simulation with rainfall inputs that were particularly higher for June, July, and August.

Table 3. Mean monthly solar radiation, maximum and minimum temperatures, and monthly total rainfall in 1997 and 1998 at Nyankpala, Tamale, Ghana.

Month	Solar radiation	Maximum temperature	Minimum temperature	Rainfall
	MJ m^{-2} d^{-1}	°C		mm
		1997		
Jan.	17.0	36.2	20.4	0
Feb.	14.9	36.4	19.9	0
Mar.	17.6	37.7	24.1	30.5
Apr.	20.4	35.1	23.8	120.3
May	19.8	32.6	22.7	147.9
June	17.4	31.1	22.5	155.8
July	15.2	29.8	22.5	136.6
Aug.	16.7	31.0	22.6	172.8
Sept.	17.4	31.3	22.7	255.8
Oct.	18.2	32.8	22.9	137.1
Nov.	20.5	35.0	22.2	0.5
Dec.	14.8	35.9	19.6	0
		1998		
Jan.	15.6	36.3	18.3	0
Feb.	20.7	38.7	23.5	0
Mar.	17.1	39.6	25.2	0
Apr.	17.7	38.1	26.8	8.7
May	17.2	34.5	24.5	116.5
June	16.8	31.5	24.5	101.8
July	16.0	30.9	25.2	105.6
Aug.	14.3	29.8	25.1	128.9
Sept.	15.4	30.2	26.0	282.8
Oct.	19.1	32.3	25.0	75.5
Nov.	21.5	35.8	22.1	6.0
Dec.	17.4	34.9	19.8	2.4

Soil Water Dynamics

Measured and modeled soil water content in various layers of the soil profile are shown for the first sowing date of the 1998 season (Fig. 1 and 2). During 1998, the crop was exposed to several periods of water deficits after 45 d from sowing that caused gradual depletion of water from the deeper layers (30–90 cm) over a 60-d period. As expected, soil water changes were more dynamic in the top 30-cm soil layer than in the subsoil. There was negligible soil water uptake from the 90- to 113-cm soil layer (data not presented).

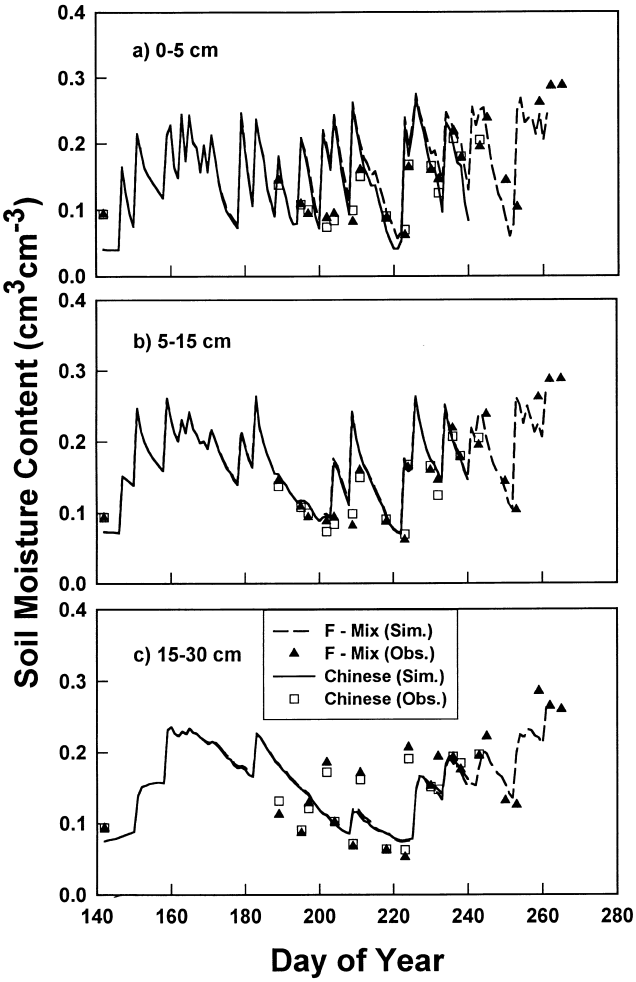

Fig. 1. Simulated and measured soil water content in the 0- to 30-cm soil profile during the growing season of peanut sown on 22 May 1998. Root mean square error value was 0.0859, 0.0583, and 0.0483 cm cm^{-3} for 0- to 5-, 5- to 10-, and 15- to 30-cm depths, respectively. Willmott (1981) index of agreement (*d* value) was 0.513, 0.676, and 0.739 for 0- to 5-, 5- to 10-, and 15- to 30-cm depths, respectively.

Reproduced from Agronomy Journal. Published by American Society of Agronomy. All copyrights reserved.

The model accurately simulated the changes in soil water content in various layers of soil profile (Fig. 1 and 2) but was less accurate for the 0- to 15- and 15- to 30-cm soil layers where more fluctuation in soil water content occurred. These were also the layers sampled by gravimetric methods. For the soil layers above 30 cm, the RMSE was between 0.0483 and 0.0859 cm cm^{-3}, and the *d* value was 0.513 to 0.739. On several dates (Days 202, 211, and 224), it appears that water actually infiltrated to the 15- to 30-cm zone after rain events of 9, 31, and 23 mm occurring on Days 201, 211, and 223, respectively, but the water balance model did not simulate this. Model failure to predict this infiltration was initially hypothesized to be caused by too much simulated runoff (too high CN number), but the simulated runoffs were less than 10% of the rainfall amounts for those dates. Too high prediction of evaporation or transpiration during the incomplete canopy phase could also be a cause for failure of infiltration from the 0- to 15-cm layer. Below 30-cm depth, predictions of soil water dynamics were close to observed data, resulting in low RMSE (0.0055 to 0.0135 cm cm^{-3}) and high *d* values (0.836 to 0.950). The two cultivars did not differ in soil water extraction during the season, except that F-mix, being a long-duration cultivar, continued to extract water after harvest of the Chinese cultivar.

The above results indicate that calibration of the model for various soil parameters such as U, CN2, SWCON, DUL, LL, and rooting (WR) parameters resulted in satisfactory soil water balance. The model also simulated the soil water balance satisfactorily for other sowing dates except late in the year when the crops were damaged by foliar diseases. In such cases, the model underestimated soil water content because the modeled crop continued soil water extraction while water extraction did not occur because disease apparently damaged the crop, reducing transpiration.

Plant Extractable Soil Water

As there was practically no water uptake by the crop from soil layers below 90-cm depth, the changes in PESW during the 1998 season for the four sowing dates are presented for the top 90-cm soil depth only (Fig. 3).

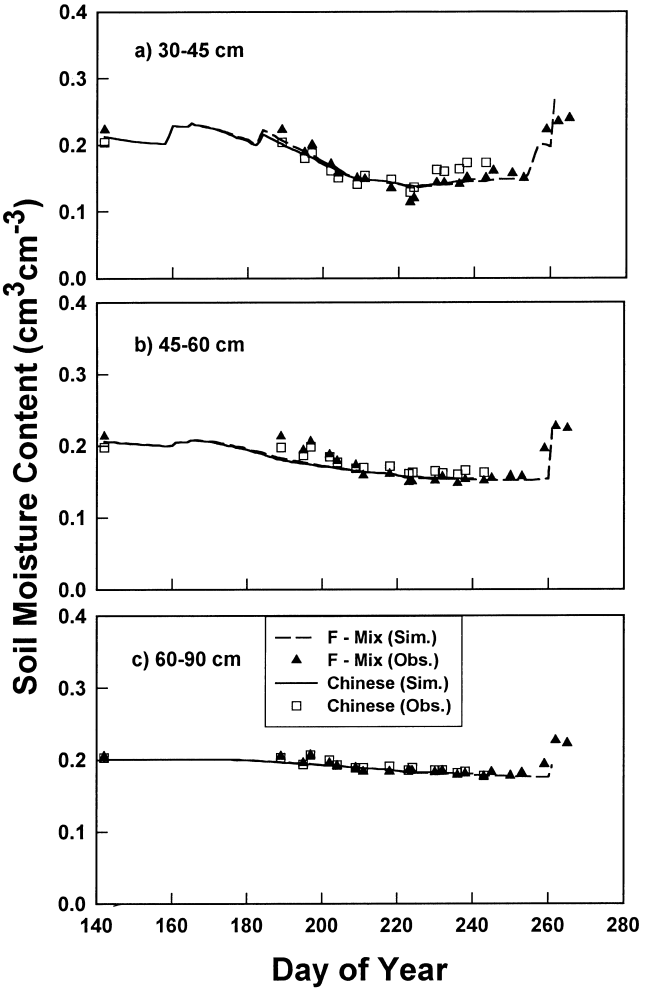

Fig. 2. Simulated and measured soil water content in the 30- to 90-cm soil profile during the growing season of peanut sown on 22 May 1998. The root mean square error was 0.0115, 0.0135, and 0.0055 cm cm^{-3} while the *d* value was 0.950, 0.836, and 0.877 for 30- to 45-, 45-to 60-, and 60- to 90-cm depths, respectively.

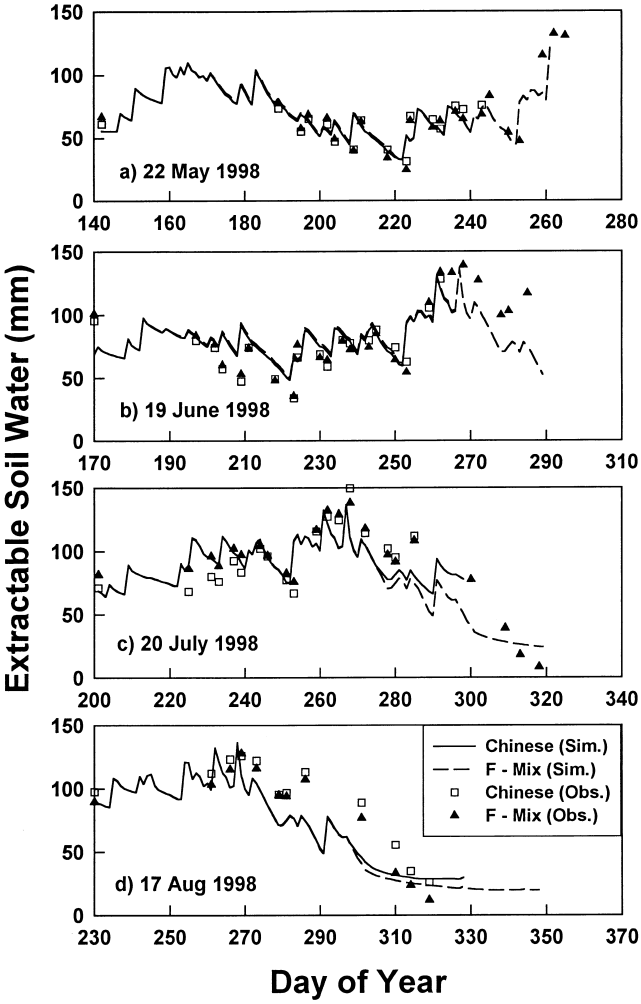

Fig. 3. Simulated and measured plant extractable soil water in the top 90 cm of soil for the four sowing dates during the 1998 season. The root mean square error was 14.3, 20.8, 18.5, and 20.8 mm while the *d* value was 0.707, 0.728, 0.870, and 0.907 for sowing on 22 May, 19 June, 20 July, and 17 August, respectively.

Reproduced from Agronomy Journal. Published by American Society of Agronomy. All copyrights reserved.

The crop sown 22 May suffered from a few days of water deficit during midseason when PESW had fallen to 31% of available and model simulation induced 50 to 60% reduction in transpiration. The model simulated dynamics of PESW during periods of soil water accretion and depletion fairly accurately (*d* values of 0.707 to 0.907), indicating that once the soil parameters were calibrated, the model was accurate in simulating the whole profile soil water dynamics under the peanut crop. Changes in PESW were also accurately simulated for other sowing dates for both cultivars, except late in the growing season of the third and fourth sowing dates. This was attributed to foliar diseases that were more pronounced with later sowings and caused decreased leaf mass and poor shoot and root growth, leading to less transpiration and water uptake by the crop.

Pod Harvest Index

Pod harvest index is the ratio of pod mass to total aboveground mass and is a good indicator of onset and intensity of partitioning to reproductive. It is a more reliable indicator because there is less error (and higher *d* values) for prediction of pod harvest index (Fig. 4 and 5) than for prediction of absolute pod mass. Knowing and predicting the date of first flowering was inadequate for setting partitioning parameters related to timing and rate of pod addition. The comparison of simulated vs. observed pod harvest index (Fig. 4 and 5) was used to help set the genetic coefficients that describe the photothermal time from flowering to first pod (FL-SH), from flowering to first seed (FL-SD), the duration of pod addition (PODUR), and partitioning intensity (XFRUIT). These first three are life cycle phase durations that influence the onset of rapid increase in pod harvest index, whereas partitioning intensity represents the maximum fraction of daily instantaneous assimilate allowed to go to pods plus seeds and thus influences the final magnitude of pod harvest index. The Chinese cultivar began forming pods earlier (7 vs. 8.8 PD), began seed growth earlier (17.5 vs. 19.0 PD), and set its pods in a shorter period (14 vs. 25 PD) than did F-mix (Table 2). The cultivars in this study had partitioning coefficients of 0.78 for Chinese and 0.77 for F-mix. For comparison, partitioning coefficient for soybean cultivars is 1.00 (Boote et al., 1998). Using the same cultivar coefficients as used for 1997, the pod harvest indices of cultivars were simulated for the 1998 season (Fig. 4 and 5). Predictions of pod harvest index for 1998 were acceptable for F-mix but not as good for the Chinese cultivar, particularly at later sowing dates when the model overpredicted.

Leaf Weight Predictions and Evidence of Disease-Induced Defoliation

Figures 6 and 7 show changes in leaf dry weight with time. The model predicted leaf dry weight fairly well

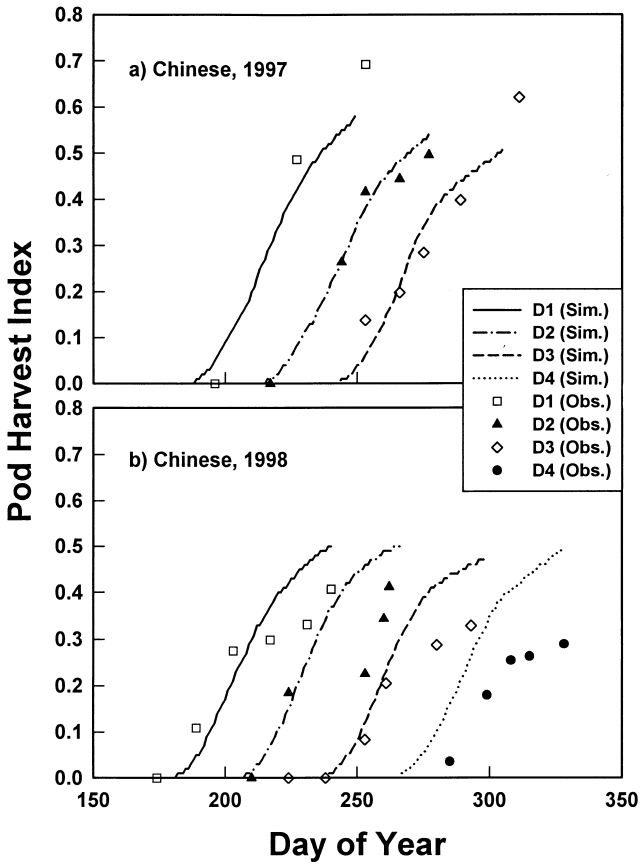

Fig. 4. Simulated and observed pod harvest index of cultivar Chinese for various sowing dates during the 1997 and 1998 seasons. The root mean square error was 0.0993, and the *d* value was 0.921 averaged over all dates and years.

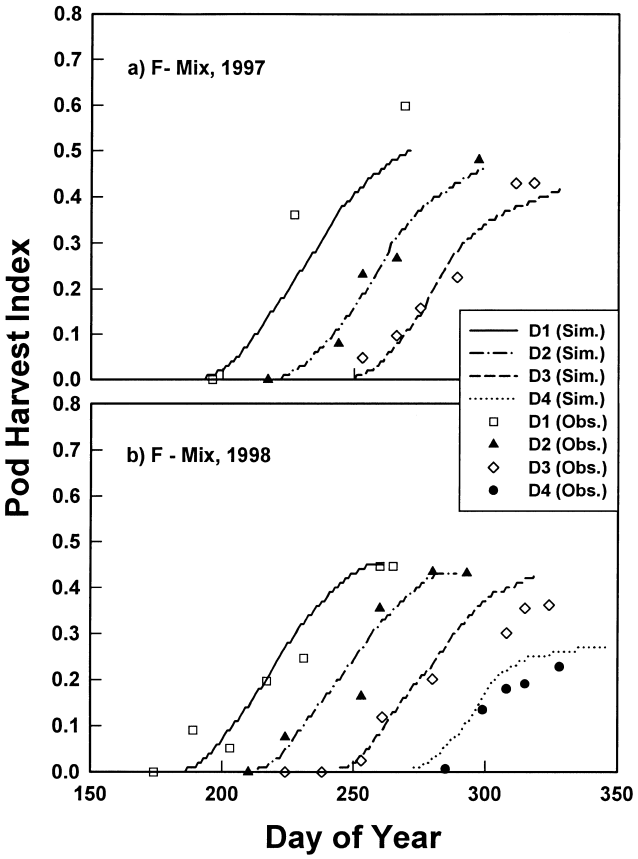

Fig. 5. Simulated and observed pod harvest index of cultivar F-Mix for various sowing dates during the 1997 and 1998 seasons. The RMSE was 0.0510, and the *d* value was 0.975 averaged over all dates and years.

Reproduced from Agronomy Journal. Published by American Society of Agronomy. All copyrights reserved.

until 65 d after sowing for Chinese and up to 75 d for F-mix when leaf dry weight began to decline. Modeled leaf mass does not normally decline much because peanut leaves stay green and remain on the plant if protected from leaf diseases and insects (the model assumes no insect defoliation or leaf diseases). However, no disease control measures were used in the present experiment. The decline in leaf weight was attributed to diseases such as late leafspot, which is a common occurrence in this environment. Late leafspot incidence was observed but not quantified in this study; thus, other leaf diseases could also have contributed to defoliation. To account for the effects of disease and associated leaf defoliation, we used functions in the model that create photosynthesis losses due to loss of leaf area and due to increase in visible percentage disease (Boote et al., 1983, 1993; Batchelor et al., 1993). We input variable defoliation across time to mimic the observed decline in leaf weight from the peak leaf mass at mid–life cycle to values observed at the end of the season. The percentage defoliation at maturity required to mimic the observed decline in leaf weight resulted in less than 25% defoliation for the first planting dates, increasing up to 75% for later planting dates. This is consistent with increasing disease pressure later in the season. We also input percentage visible leafspot disease, starting at zero at mid–life cycle (at 42 to 62 d after sowing, onset being earlier with later sowing date and varying with year) and increasing to a maximum of 10 to 15% necrosis at the end of the season, similar to the pattern observed by Bourgeois et al. (1991). We used a virtual lesion ratio of 4.0 in the model, as estimated by Bourgeois and Boote (1992) for leafspot necrosis effect on peanut leaf photosynthesis, meaning there is an effective four-unit decrease in green photosynthesizing leaf area for every one unit of necrotic diseased area (Bastiaans, 1991). With these changes, the model simulated the decline in leaf weight (Fig. 6 and 7) and also the late-season decreases in total biomass accumulation. With the defoliation and necrosis function, the RMSE for leaf mass was 254 kg ha^{-1}, and the *d* value was 0.937, averaged over 2 yr. Without it, the RMSE was 581 kg ha^{-1}, and the *d* value was 0.740.

Accounting for Defoliation Effects on Predictions of Total Biomass and Pod Weight

Figures 8 to 11 show model predictions of total biomass and pod dry weights, with and without the defoliation function, of both cultivars for the first (D1) and the third (D3) sowing dates in 1997 and 1998 (results

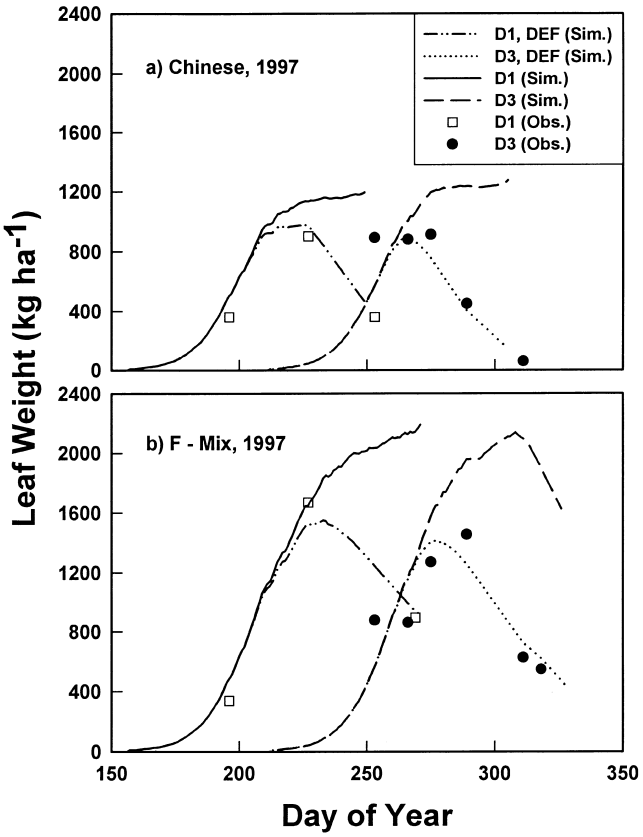

Fig. 6. Simulated and observed leaf mass of two cultivars, with and without defoliation function (DEF), for the first (D1) and third (D3) sowing dates during the 1997 season. With the defoliation function and over both dates and cultivars, the root mean square error (RMSE) was 195 kg ha^{-1}, and the *d* value was 0.949. Without the defoliation function, the RMSE was 725 kg ha^{-1}, and the *d* value was 0.561.

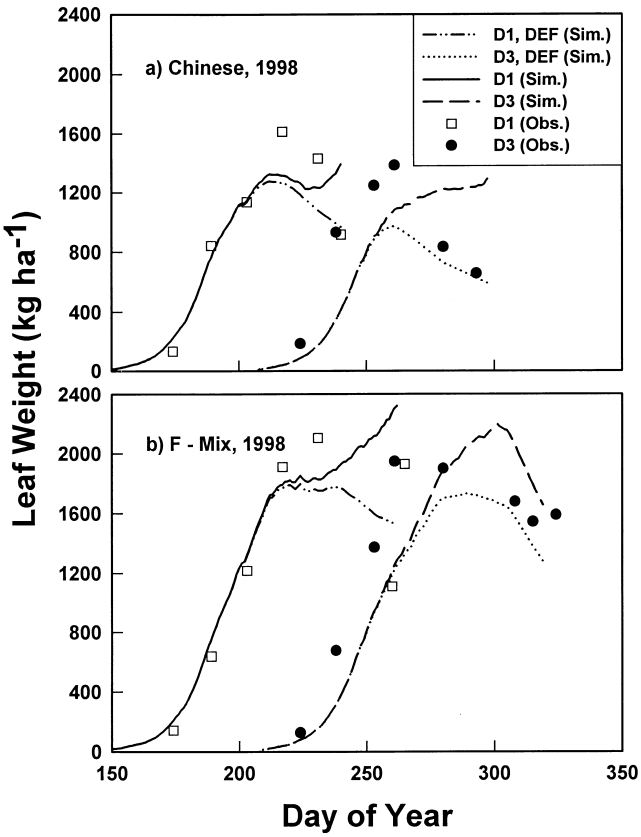

Fig. 7. Simulated and observed leaf mass of two cultivars, with and without defoliation function (DEF), for the first (D1) and third (D3) sowing dates during the 1998 season. With the defoliation function and over both dates and cultivars, the root mean square error (RMSE) was 302 kg ha^{-1}, and the *d* value was 0.925. Without the defoliation function, the RMSE was 386 kg ha^{-1}, and the *d* value was 0.896.

Reproduced from Agronomy Journal. Published by American Society of Agronomy. All copyrights reserved.

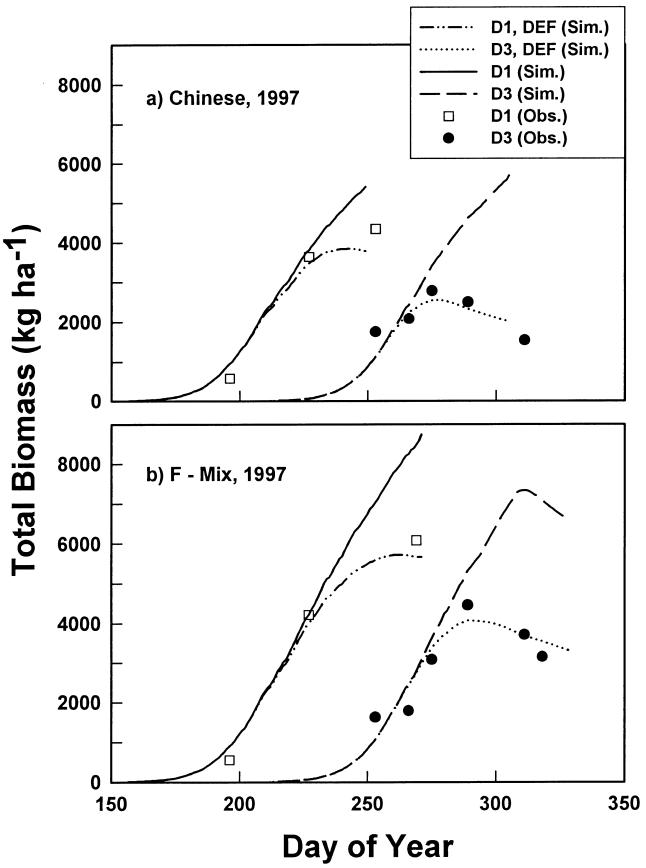

Fig. 8. Simulated and observed total biomass of two cultivars, with and without defoliation function (DEF), for the first (D1) and third (D3) sowing dates during the 1997 season. With the defoliation function and over both dates and cultivars, the root mean square error (RMSE) was 395 kg ha^{-1}, and the *d* value was 0.979. Without the defoliation function, the RMSE was 1875 kg ha^{-1}, and the *d* value was 0.763.

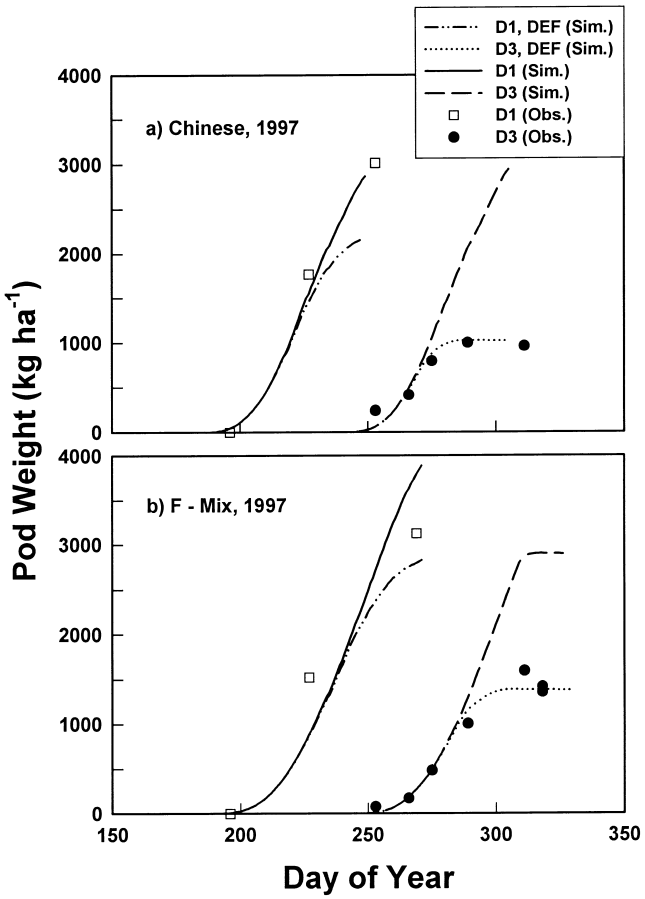

Fig. 9. Simulated and observed pod mass of two cultivars, with and without defoliation function (DEF), for the first (D1) and third (D3) sowing dates during the 1997 season. With the defoliation function and over both dates and cultivars, the root mean square error (RMSE) was 284 kg ha^{-1}, and the *d* value was 0.971. Without the defoliation function, the RMSE was 826 kg ha^{-1}, and the *d* value was 0.849.

for D2 and D4 sowing dates are not shown because they are similar to results of D1 and D3). Without the defoliation inputs, the model predicted biomass and pod production accurately up to 75 and 80 d after sowing for Chinese and F-mix in 1997, and after that date, it overpredicted both components, with high RMSE (1875 and 826 kg ha^{-1} for biomass and pod, averaged over dates and cultivars) and only moderate *d* value (0.763 and 0.849 for biomass and pod). With the defoliation function, there was considerable improvement of model prediction in 1997 (Fig. 8 and 9), giving much lower RMSE (395 and 284 kg ha^{-1} for biomass and pod) and higher *d* value (0.979 and 0.971 for biomass and pod). Similarly, the model predicted biomass and pod dry weight in 1998 accurately up to 80 and 100 d after sowing for Chinese and F-mix, respectively, and overpredicted thereafter (Fig. 10 and 11). With the defoliation inputs to the model, there was clear improvement of prediction of biomass (RMSE decreased from 848 to 587 kg ha^{-1}) and pod mass (RMSE decreased from 455 to 221 kg ha^{-1}) in 1998. The improvements in prediction of biomass and pod yield during the last half of the growing cycle were not a result of calibrating to those tissues but rather were automatically produced by the crop growth model as a consequence of the reduction in leaf area index (light interception) and the imposition of necrotic (nonphotosynthetic) tissue. The slopes of total biomass increase and pod mass increase, which were initially too steep without the disease function, were decreased approximately 25 and 28%, respectively, on average by that function although the reduction in pod yield was larger, especially for later sowing dates. Without the disease function, the model tended to increasingly overpredict total crop and pod growth for later sowing dates, regardless of cultivar and year. This was particularly true for the third planting date in 1997 and the fourth date in 1998 and was consistent with increased disease severity toward the end of the humid rainy season.

Improved Predictions of Pod Yield and Final Biomass after Accounting for Disease Effects

The productivity of later sowing dates was more affected by disease and defoliation inputs than that of early sowing dates (Table 4), also confirmed by the loss in leaf mass that is characteristic of leafspot disease (Fig. 6 and 7). Once these disease and defoliation effects were accounted for in the CROPGRO-peanut model,

Reproduced from Agronomy Journal. Published by American Society of Agronomy. All copyrights reserved.

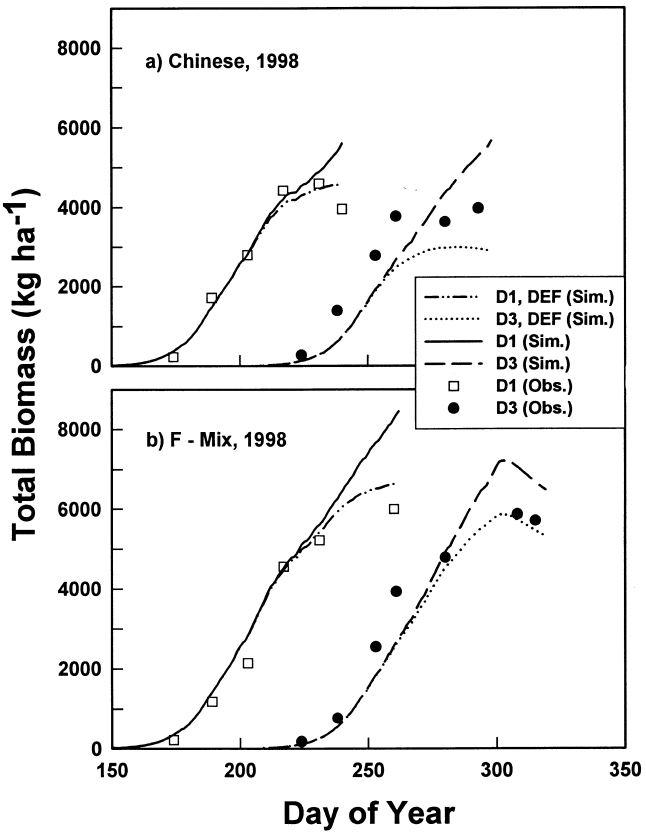

Fig. 10. Simulated and observed total biomass of two cultivars, with and without defoliation function (DEF), for the first (D1) and third (D3) sowing dates during the 1998 season. With the defoliation function and over both dates and cultivars, the root mean square error (RMSE) was 587 kg ha^{-1}, and the *d* value was 0.976. Without the defoliation function, the RMSE was 848 kg ha^{-1}, and the *d* value was 0.959.

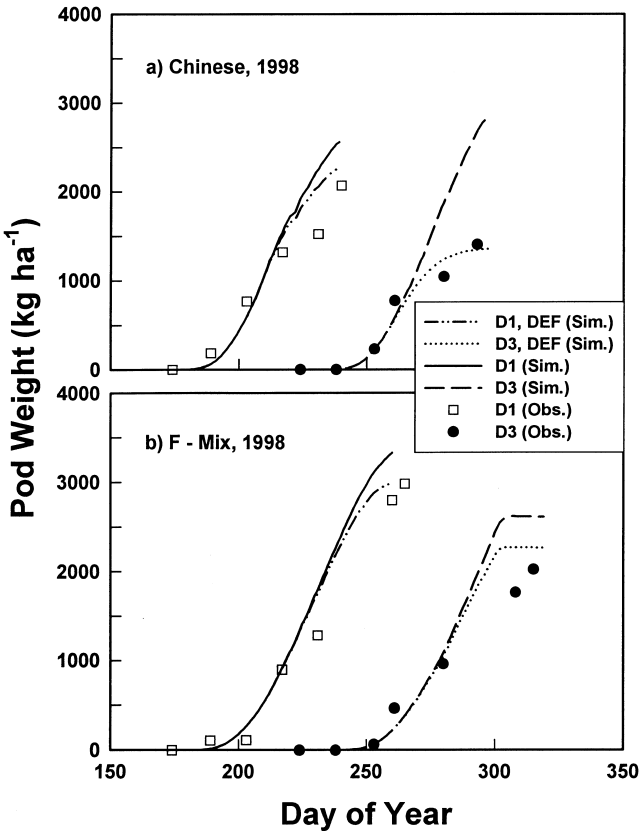

Fig. 11. Simulated and observed pod mass of two cultivars, with and without defoliation function (DEF), for the first (D1) and third (D3) sowing dates during the 1998 season. With the defoliation function and over both dates and cultivars, the root mean square error (RMSE) was 221 kg ha^{-1}, and the *d* value was 0.984. Without the defoliation function, the RMSE was 455 kg ha^{-1}, and the *d* value was 0.945.

the simulated biomass and pod and seed yields were close to the observed yields for all sowing dates in both seasons. After accounting for disease effects, the respective *d* values were 0.833, 0.858, and 0.844 for prediction of total biomass, pod yield, and seed yield, respectively (Table 4). Considering only water limitations on pod yield resulted in overpredictions (2804 predicted vs. 1726 kg ha^{-1} observed average), with higher RMSE (1362 vs. 622 kg ha^{-1}) and lower *d* value (0.619 vs. 0.858). From R^2 of linear regressions of predicted vs. observed pod yield (regressions not shown), we estimate that the crop model accounted for 34% of pod yield variation considering only weather and soil water but 63% of yield variation if disease effects were considered along with weather and soil water. This highlights the importance, in model predictions of yield, of accounting for biotic factors along with weather factors.

Yield Potential and Yield Reductions (Gaps) from Water Deficit and Pests

First, the simulations were run for growing conditions with water balance and pest damage inputs "turned off" to estimate the climatic yield potential. Then reductions caused by water deficit were simulated for growing conditions with water balance turned "on" but with pest damage inputs still "turned off" (Table 5). Average yield reductions due to water deficit were small for the early two sowing dates (averaging 5 to 10%) but increased with delay in sowing to 20% for the third date and 70% for the fourth date (1998 only). Average yield loss from biotic factors of all types (reduction in observed yield, expressed as a percentage decline from water-limited simulated yield) was 40%, increasing with delayed sowing, averaging 11, 52, 48, and 61% for the successive four sowing dates. Yield reductions (gaps) attributed to biotic stresses were generally greater for cultivar Chinese than with cultivar F-mix, increasing with delayed sowing dates. Because of its longer life cycle, F-mix had a higher simulated climatic yield potential than Chinese, as confirmed by the higher observed yields of F-mix, especially with earlier sowings. Also because of its longer life cycle, F-mix had greater yield reductions under water-limiting conditions, especially for later sowing dates. Because of these two compensating effects (Chinese more affected by biotic stresses and F-mix more affected by water limitation), the total yield reductions attributed to both water deficit and biotic stresses were generally similar for Chinese (25 to 88%) and F-mix (24 to 91%). Yield gap from low soil fertility, while not

Reproduced from Agronomy Journal. Published by American Society of Agronomy. All copyrights reserved.

Table 4. Simulated and observed total crop biomass, pod yield, and seed yield of cultivars in 1997 and 1998 at Nyankpala, Tamale, Ghana, when defoliation function is considered along with weather and soil water effects. Root mean square errors of simulated vs. observed total biomass, pod yield, and seed yield were 1385, 622, and 496 kg ha^{-1}, respectively. The *d* value was 0.833, 0.858, and 0.844 for total biomass, pod yield, and seed, respectively.

	Total biomass		Pod yield		Seed yield	
Sowing date	Simulated	Observed	Simulated	Observed	Simulated	Observed
	kg ha^{-1}					
			Chinese			
29 May 1997	3791	4353	2182	3163	1572	2460
26 June 1997	2855	3061	1532	1484	987	928
24 July 1997	2014	1550	1021	740	593	492
			F-mix			
29 May 1997	5671	6085	2823	3124	2054	2102
26 June 1997	4285	2885	1976	2029	1312	1331
24 July 1997	3292	3161	1380	1421	857	1008
			Chinese			
22 May 1998	4570	5091	2289	2072	1694	1491
19 June 1998	3855	3357	1933	1383	1401	943
20 July 1998	2896	1897	1361	624	968	426
17 Aug. 1998	2145	1378	1055	400	675	286
			F-mix			
22 May 1998	6662	6691	3001	2984	2223	2126
19 June 1998	6936	3302	2971	1423	2215	968
20 July 1998	5309	8127	2268	2942	1537	2117
17 Aug. 1998	2599	1662	715	379	359	240

Table 5. Simulated pod yield reductions attributed to water deficit and biotic stress factors by comparison to observed pod yields of two cultivars sown on selected dates in 1997 and 1998 at Nyankpala, Tamale, Ghana.

	Pod yield			Yield reduction		
Sowing date	Water nonlimiting (simulated) (*A*)	Water limiting (simulated) (*B*)	Observed yield (*C*)	Yield reduction due to water limitation $100 \times (A - B)/A$	Yield reduction due to biotic stress $100 \times (B - C)/B$	Yield reduction from both factors $100 \times (A - C)/A$
	kg ha^{-1}			%		
			Chinese			
29 May 1997	2952	2866	3163	3	−10	−7
26 June 1997	3076	2972	1484	3	50	52
24 July 1997	3048	2941	740	4	75	76
			F-Mix			
29 May 1997	4330	3889	3124	10	20	28
26 June 1997	4316	3925	2029	9	48	53
24 July 1997	4587	2894	1421	37	51	69
			Chinese			
22 May 1998	2776	2575	2072	7	20	25
19 June 1998	2869	2840	1383	1	51	52
20 July 1998	2800	2857	624	−2	78	78
17 Aug. 1998	3274	1300	400	60	69	88
			F-Mix			
22 May 1998	3916	3382	2984	14	12	24
19 June 1998	3640	3388	1423	7	58	61
20 July 1998	4264	2611	2942	39	−13	31
17 Aug. 1998	4295	814	379	81	53	91

addressed explicitly in Table 5, can be implied from the degree to which the fertility factor (SLPF) was decreased from 0.92 (for productive peanut soils in Florida) to 0.86 value for this study (to fit early linear phase of dry matter accumulation).

Long-Term Analysis of Crop Yields

Rainfall limitations can be better evaluated by averaging simulations from many weather years. Seed yield was simulated under three scenarios, i.e., water nonlimiting, water limiting, and both water and pests limiting, using weather data from each of 13 yr (1986 to 1998) and results averaged for Table 6. Under water nonlimiting situation, the potential mean yield of the short-duration cultivar Chinese varied from 2123 to 2364 kg ha^{-1}, and the potential mean yield of F-Mix varied from 2904 to 3304 kg ha^{-1} (Table 6). These minor sowing date effects on potential yield for water nonlimiting conditions are attributed to small differences in solar radiation and temperature. Most important, they illustrate that actual yield variation with sowing date must be related to either soil water deficit or to increased incidence of disease and pests, rather than inadequate solar radiation or stressful temperature.

Under water-limiting conditions (actual weather of 13 yr), the potential yield of Chinese increased from 1919 to 2158 kg ha^{-1} when sowing was delayed from 22 May to 20 July (Table 6). With further delay in sowing,

Reproduced from Agronomy Journal. Published by American Society of Agronomy. All copyrights reserved.

Table 6. Simulation analysis of seed yields of Chinese and F-Mix cultivars under various yield-limiting conditions. Simulated for 13 yr of weather (1986 to 1998) at Nyankpala, Tamale, Ghana, and reported as mean yield over 13 yr.

	Seed yield				
Sowing date	Mean	Yield loss as percentage of potential mean yield†	Standard deviation	Minimum	Maximum
	kg ha^{-1}	%	kg ha^{-1}		
Chinese; water nonlimiting					
22 May	2123	–	119	1932	2354
19 June	2122	–	183	1819	2394
20 July	2339	–	161	2050	2619
17 Aug.	2364	–	102	2195	2501
Chinese; water limiting					
22 May	1919	10	299	1227	2288
19 June	2029	4	239	1638	2354
20 July	2158	8	203	1735	2391
17 Aug.	882	63	337	418	1777
Chinese; water limiting and pest‡					
22 May	1673	21	256	1109	2038
19 June	1333	37	109	1153	1490
20 July	958	59	74	825	1065
17 Aug.	614	74	132	398	735
F-Mix; water nonlimiting					
22 May	2904	–	230	2648	3344
19 June	3123	–	316	2583	3453
20 July	3304	–	205	2940	3555
17 Aug.	3124	–	166	2782	3302
F-Mix; water limiting					
22 May	2557	12	306	2015	3194
19 June	2722	13	302	2199	3269
20 July	1925	42	383	1200	2697
17 Aug.	549	82	177	362	1047
F-Mix; water limiting and pests‡					
22 May	2295	21	227	1849	2755
19 June	2346	25	205	1951	2663
20 July	1634	51	269	1092	2049
17 Aug.	457	85	174	232	936

† Percentage of water nonlimiting mean yield for each sowing date and cultivar.

‡ Pest simulation used the disease functions (defoliation and necrosis) derived for actual sowing dates in each year; however, Table 6 makes no use of observed yields.

the yields decreased because decreased rainfall during the crop growth cycle caused soil water deficits during the reproductive phase (Table 7). Yield loss caused by water deficits for Chinese ranged from 4 to 63% of the potential yields simulated for the respective sowing dates (Table 6). For F-Mix, high seed yield of 2557 to 2722 kg ha^{-1} was simulated up to 19 June sowing date, but further delay in sowing decreased yields substantially because of decrease in water availability (Table 7). Yield loss caused by water deficits for F-Mix ranged from 12 to 82% of the potential yields simulated for the respective sowing dates.

When both water and pests were limiting, using disease functions (defoliation and necrosis) from actual 1998 sowing dates (applied to these 13 yr), the simulated seed yield of Chinese ranged from 1673 to 614 kg ha^{-1}, declining with delay in sowing. These values represent 79 to 26% of the potential yields (or 21 to 74% yield loss) simulated for the respective sowing dates. For F-Mix, the yields ranged from 2295 to 457 kg ha^{-1}, declining with delay in sowing, which represented 79 to 15% of the potential yields (or 21 to 85% yield loss) simulated for the respective sowing dates.

Table 7. Mean rainfall and its standard deviation (SD) for 1986 to 1998 during the growing period of cultivars Chinese and F-Mix associated with four selected sowing dates.

	Seasonal rainfall			
	Chinese		F-Mix	
Sowing date	Mean	SD	Mean	SD
	mm			
22 May	533	197	720	260
19 June	607	232	713	235
20 July	562	164	576	159
17 Aug.	456	140	461	136

The above analysis of the long-term yield simulations showed that F-Mix, being a long-duration crop, has higher yield potential than Chinese. The yields under both water and biotic stress limitations are higher for F-Mix only for the first three sowing dates (22 May, 19 June, and 20 July) compared with Chinese. The results also indicate that when peanut is sown late under rainfed conditions in Ghana, the control of diseases is necessary to realize the yield potential.

CONCLUSIONS

Field studies of three or four sowing dates using two peanut cultivars in northern Ghana showed that yields were highest for early sowing and declined consistently with later sowing. Weather, soil water measurements, and crop growth measurements were collected during the season and evaluated by comparison to crop growth simulations to evaluate possible causes for the decline in growth and yield with later sowing dates. The CROPGRO-peanut model was able to simulate crop growth, dry matter partitioning, and yields at final harvest fairly well for early sowings in both years but overestimated growth and yield for later sowing dates even when soil water deficits were accounted for. Later sowings had damage to the crop caused by diseases and pests that increased with the delay in sowing. After incorporating percentage diseased leaf area and percentage leaf defoliation information, simulations of leaf mass, crop growth, and pod yield improved. Simulation of yields for water-limiting compared with water nonlimiting conditions for the two seasons showed that the simulated hypothetical yield loss from water deficit was small for the first two sowing dates (1–14%, 7% on average) but was larger (20 and 70%) for the third and fourth sowing dates, respectively. When sown on these two later dates, F-mix had greater exposure to drought, with greater hypothetical yield losses from water deficit (ranging from 37 to 81% compared with 4 to 60% for Chinese). With delay in sowing, the yields of both cultivars were also decreased by biotic stresses, especially by late leafspot. Average yield loss from biotic stress was 40%, being as low as 11% for the earliest date and as high as 61% for the fourth date. Maximum yield loss caused by biotic stress, when expressed as percentage of water-limited yield, was as high as 78% for Chinese and 58% for F-Mix. Total yield reduction because of both water and

biotic stresses ranged from 25 to 88% for Chinese and 24 to 91% for F-Mix for different sowing dates during the two seasons. Simulation with long-term historical weather data confirmed these yield reductions attributable to water deficit and biotic stresses for the sowing dates. These systems analyses led us to recommend future fungicide trials to test the degree of yield enhancement possible if diseases were controlled with fungicides. We conclude from this study that the CROPGRO-peanut model is a useful tool for quantifying potential yields and yield gaps associated with various stresses in the Guinea Savanna Zone of Ghana.

REFERENCES

Bastiaans, L. 1991. The ratio between virtual and visual lesion size as a measure to describe reduction in leaf photosynthesis of rice due to leaf blast. Phytopathology 81:611–615.

Batchelor, W.D., J.W. Jones, K.J. Boote, and H.O. Pinnschmidt. 1993. Extending the use of crop models to study pest damage. Trans. ASAE 36:551–558.

Boote, K.J. 1982. Growth stages of peanut (*Arachis hypogaea* L.). Peanut Sci. 9:35–40.

Boote, K.J., W.D. Batchelor, J.W. Jones, H. Pinnschmidt, and G. Bourgeois. 1993. Pest damage relations at the field level. p. 277–296. *In* F.W.T. Penning de Vries et al. (ed.) Systems approaches for agricultural development. Kluwer Academic Publ., Dordrecht, the Netherlands.

Boote, K.J., J.M. Bennett, J.W. Jones, and H.E. Jowers. 1989a. On-farm testing of peanut and soybean models in north Florida. Paper presented at the International Summer Meeting of the Am. Soc. of Agric. Eng. and the Can. Soc. of Agric. Eng., Quebec, Canada. 25–28 June 1989. Paper no. 894040. ASAE, St. Joseph, MI.

Boote, K.J., J.W. Jones, G. Hoogenboom, and N.B. Pickering. 1998. The CROPGRO model for grain legumes. p. 99–128. *In* G.Y. Tsuji, G. Hoogenboom, and P.K. Thornton (ed.) Understanding options for agricultural production. Kluwer Academic Publ., Dordrecht, the Netherlands.

Boote, K.J., J.W. Jones, G. Hoogenboom, G.G. Wilkerson, and S.S. Jagtap. 1989b. PNUTGRO V1.02. Peanut crop growth simulation model. User's guide. Florida Agric. Exp. Stn., Journal no. 8420. Univ. of Florida, Gainesville.

Boote, K.J., J.W. Jones, J.W. Mishoe, and R.D. Berger. 1983. Coupling pests to crop growth simulators to predict yield reductions. Phytopathology 73:1581–1587.

Boote, K.J., J.W. Jones, J.W. Mishoe, and G.G. Wilkerson. 1986. Modeling growth and yield of groundnut. p. 243–254. *In* Agrometeorology of groundnut. Proc. Int. Symp., ICRISAT Sahelian Center, Niamey, Niger. 21–26 Aug. 1985. ICRISAT, Patancheru, Andhra Pradesh, India.

Boote, K.J., J.W. Jones, and N.B. Pickering. 1996. Potential uses and limitations of crop models. Agron. J. 88:704–716.

Boote, K.J., J.W. Jones, and P. Singh. 1991. Modeling growth and yield of groundnut—state of the art. p. 331–343. *In* S.N. Nigam (ed.) Groundnut—a global perspective. Proc. Int. Workshop, ICRISAT Center, Patancheru, AP, India. 25–29 Nov. 1991. ICRISAT, Patancheru, AP, India.

Bourgeois, G., and K.J. Boote. 1992. Leaflet and canopy photosynthesis of peanut affected by late leaf spot. Agron. J. 84:359–366.

Bourgeois, G., K.J. Boote, and R.D. Burger. 1991. Growth, development, yields, and seed quality of Florunner peanut affected by late leaf spot. Peanut Sci. 18:137–143.

FAO. 1997. FAO production yearbook. Vol. 51. FAO Stat. Ser. 149. Food and Agric. Organ. of the United Nations, Rome.

Gilbert, R.A. 1992. On-farm testing of the PNUTGRO crop model in Florida. M.S. thesis. Univ. of Florida, Gainesville.

Gilbert, R.A., K.J. Boote, and J.M. Bennett. 2002. On-farm testing of the PNUTGRO crop growth model in Florida. Peanut Sci. 29: 58–65.

Hansen, J.W., N.B. Pickering, J.W. Jones, C. Wells, H.V.K. Chan, and D.C. Godwin. 1994. Managing and generating daily weather data. p. 137–200. *In* G.Y. Tsuji, G. Uehara, and S. Balas (ed.) DSSAT V3. Vol. 3–3. Univ. of Hawaii, Honolulu.

Hoogenboom, G., J.W. Jones, and K.J. Boote. 1992. Modeling growth, development, and yield of grain legumes using SOYGRO, PNUTGRO, and BEANGRO: A review. Trans. ASAE 35:2043–2056.

Hoogenboom, G., J.W. Jones, K.J. Boote, W.T. Bowen, N.B. Pickering, and W.D. Batchelor. 1993. Advancement in modeling grain legume crops. Paper no. 93–4511. ASAE, St. Joseph, MI.

Hoogenboom, G., J.W. Jones, P.W. Wilkens, W.D. Batchelor, W.T. Bowen, L.A. Hunt, N.B. Pickering, U. Singh, D.C. Godwin, B. Baer, K.J. Boote, J.T. Ritchie, and J.W. White. 1994. Crop models. p. 95–244. *In* G.Y. Tsuji, G. Uehara, and S. Balas (ed.). DSSAT Version 3. Volume 2. Univ. of Hawaii, Honolulu.

[IBSNAT] International Benchmark Sites Network for Agrotechnology Transfer Project. 1989. Decision Support System for Agrotechnology Transfer Version 2.1 (DSSAT V2.1). Dep. of Agron. and Soil Sci., College of Trop. Agric. and Human Resour., Univ. of Hawaii, Honolulu.

Priestley, C.H.B., and R.J. Taylor. 1972. On the assessment of surface heat flux and evaporation using large-scale parameters. Mon. Weather Rev. 100:81–92.

Ritchie, J.T. 1985. A user-oriented model of the soil water balance in wheat. p. 293–305. *In* E. Fry and T.K. Atkin (ed.) Wheat growth and modeling. NATO-ASI Ser. Plenum Publ. Corp., New York.

Singh, P., K.J. Boote, A. Yogeswara Rao, M.R. Iruthayaraj, A.M. Sheikh, S.S. Hundal, R.S. Narang, and P. Singh. 1994. Evaluation of the groundnut model PNUTGRO for crop response to water availability, sowing dates, and seasons. Field Crops Res. 39:147–162.

Willmott, C.J. 1981. On the validation of models. Phys. Geogr. 2:184–194.

Reproduced from Agronomy Journal. Published by American Society of Agronomy. All copyrights reserved.